

Studies on the structural diversity of MOFs containing octahedral siloxane-backboned connectors

Luke C. Delmas^a, Peter N. Horton^b, Andrew J.P. White^a, Simon J. Coles^b, Paul D. Lickiss^a, Robert P. Davies^{a,*}

^a Department of Chemistry, Imperial College London, South Kensington, London SW7 2AZ, UK

^b EPSRC Crystallographic Service, Department of Chemistry, University of Southampton, Highfield, Southampton SO17 1BJ, UK

ARTICLE INFO

Article history:

Received 21 June 2018

Accepted 19 September 2018

Available online 27 September 2018

Keywords:

Siloxane

Polytopic linkers

MOFs

Metal–organic frameworks

Hybrid materials

ABSTRACT

Four metal–organic frameworks containing hexatopic connectors have been prepared and structurally characterised: $[\text{Cd}_3(\mathbf{L})(\text{DMA})_2(\text{H}_2\text{O})_2]$ (**IMP-28**), $[\text{Ce}_2(\mathbf{L})(\text{DMF})_2(\text{H}_2\text{O})_2]$ (**IMP-29**), $[\text{Y}_2(\mathbf{L})(\text{DMF})_2(\text{H}_2\text{O})_2]$ (**IMP-30**), and $[\text{Zn}_2(\mathbf{L}-\text{H}_2)(4,4'\text{-bipy})_2]$ (**IMP-31**). All the MOFs have been constructed using the hybrid inorganic–organic siloxane linker hexakis(4-carboxyphenyl)disiloxane ($\mathbf{L}-\text{H}_6$). In each case, discrete metal-based nodes are cross-linked by the octahedrally disposed connector to afford 3D polymeric structures. The underlying nets in these MOFs have been evaluated through deconstruction of their crystal structures and subsequent topological analysis. Examples of MOFs built from hexatopic linkers, and especially those with octahedral predispositions such as in \mathbf{L} , remain scarce and the topologies ascribed to some of these MOFs are unique.

© 2018 The Author(s). Published by Elsevier Ltd. This is an open access article under the CC BY license (<http://creativecommons.org/licenses/by/4.0/>).

1. Introduction

The field of metal–organic frameworks (MOFs) continues to flourish as the combination of new organic and inorganic building blocks affords hybrid materials [1–3] with unique properties and applications [4,5]. The discovery of new MOFs relies heavily on the design and synthesis of new linkers [6] and we have consequently focussed on the preparation of nonplanar, highly-branched, polytopic connectors starting from organosilicon reagents whose unique reactivity allows facile preparation of highly branched 3D linkers, beyond those accessible through conventional carbon-based organic chemistry [7–12]. The siloxane group (Si–O–Si) is prevalent in several types of materials including zeolites [13–15], periodic mesoporous organosilicas [16–18], POSS hybrids [19] and other porous materials [20]. Although there are numerous reported 1- and 2-dimensional coordination polymers [21–32], 3D-connected MOFs built from siloxane-based linkers remain rare [33,34]. These linkers can be considered hybrid inorganic–organic in their own right due to the presence of the inorganic siloxane backbone [33].

We recently reported the synthesis of hexakis(4-carboxyphenyl)disiloxane ($\mathbf{L}-\text{H}_6$; Fig. 1), its hydrogen-bonded superstructure, and the preparation of a porous Zn-based MOF

(**IMP-18**) derived from it [33]. Here, we further evaluate the role of this connector in MOF chemistry by reporting upon the synthesis, characterisation and topological evaluation of four new MOFs built from \mathbf{L} with a focus on the diversity of structural features with different metals. The inorganic Si–O–Si linkage in \mathbf{L} adopts a roughly linear arrangement minimizing steric interactions of the surrounding phenyl rings. This results in the coordinating carboxylate groups being disposed in a pseudo-octahedral conformation which is a rare but highly desirable [35] linker geometry for MOF construction. This has prompted us to explore thoroughly the incorporation of \mathbf{L} in novel 3D MOFs by allowing $\mathbf{L}-\text{H}_6$ to react with a variety of metal salts under solvothermal conditions. Four new MOFs have been isolated and their structures elucidated by single crystal X-ray diffraction. The underlying nets of these materials have been determined through topological analysis of their deconstructed frameworks.

2. Experimental

2.1. Materials and methods

All commercially-available chemical reagents were used as received without further purification. Hexakis(4-carboxyphenyl)disiloxane ($\mathbf{L}-\text{H}_6$) was prepared according to the literature protocol [33]. IR spectra were recorded on a Perkin Elmer instrument in the range 600–4000 cm^{-1} . Powder X-ray diffraction (PXRD) studies were performed using a Panalytical MPD X-ray diffractometer with

* Corresponding author.

E-mail addresses: p.lickiss@imperial.ac.uk (P.D. Lickiss), r.davies@imperial.ac.uk (R.P. Davies).

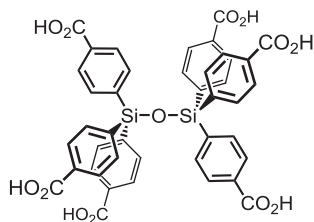


Fig. 1. Structure of hexakis(4-carboxyphenyl)disiloxane ($L-H_6$).

Cu $K\alpha$ (1.54 Å) radiation. Thermogravimetric analysis was carried out under a nitrogen atmosphere using a Mettler Toledo instrument under a constant stream of dry nitrogen gas (flow rate 50 mL min⁻¹) over the temperature range 30–800 °C and at a heating rate of 5 °C min⁻¹. X-ray data was collected using a Rigaku FRE+ (**IMP-29** and **IMP-31**), Rigaku 007HF (**IMP-30**) or Agilent Xcalibur PX Ultra (**IMP-28**) diffractometer. Solutions were solved and refined using SHELX and SHELXTL [36,37], as well as Olex-2 [38], and WinGX [39]. The SQUEEZE routine within PLATON or the solvent masking routine in Olex-2 [38] was used to remove heavily disordered solvents from the MOF structures as specified in the text [40]. Graphics were generated using the CrystalMaker software suite [41]. A summary of the crystallographic data is presented in Table 1.

2.2. Synthesis of $[Cd_3(L)(DMA)_2(H_2O)_2]$ (**IMP-28**)

$L-H_6$ (50 mg, 63 μmol) and $Cd(NO_3)_2 \cdot 4H_2O$ (58 mg, 188 μmol) were introduced into a screw-cap vial to which DMA (3.0 mL) and water (3.0 mL) were added. The mixture was agitated in an ultrasound bath for approximately 2 min with intermittent shaking to ensure complete dissolution of the reagents. The reaction mixture was gradually warmed to 85 °C using a programmable oven over a 3 h period, held at 85 °C for 42 h and allowed to cool slowly to room temperature over 3 h. Colourless crystals were isolated by suction filtration. The crystals were washed with fresh DMA (3 × 4 mL) and air dried. Yield = 40 mg (40% based on $L-H_6$).

IR (ATR): ν (cm⁻¹) = 1604, 1575, 1524, 1501, 1391, 1101, 1018, 856, 772, 732, 707.

2.3. Synthesis of $[Ce_2(L)(DMF)_2(H_2O)_2]$ (**IMP-29**)

$L-H_6$ (10 mg, 13 μmol) and $Ce(NO_3)_3 \cdot 7H_2O$ (42 mg, 113 μmol) were introduced into a screw-cap vial to which DMF (2.0 mL) and water (0.5 mL) were added. The mixture was agitated in an ultrasound bath for approximately 2 min with intermittent shaking to ensure complete dissolution of the reagents. The reaction mixture was gradually warmed to 80 °C using a programmable oven over a 3 h period, held at 80 °C for 42 h and allowed to slowly cool to room temperature over 3 h. Colourless crystals were isolated by suction filtration. The crystals were washed with fresh DMF (3 × 4 mL) and air dried. Yield = 22 mg (86% based on $L-H_6$). IR (ATR): ν (cm⁻¹) = 1645, 1576, 1529, 1496, 1403, 1358, 1252, 1103, 1064, 1017, 852, 777, 730, 707, 672, 633.

2.4. Synthesis of $[Y_2(L)(DMF)_2(H_2O)_2]$ (**IMP-30**)

$L-H_6$ (10 mg, 13 μmol) and $Y(NO_3)_3 \cdot 6H_2O$ (43 mg, 113 μmol) were introduced into a screw-cap vial to which DMF (2.0 mL) and water (0.5 mL) were added. The mixture was agitated in an ultrasound bath for approximately 2 min with intermittent shaking to ensure complete dissolution of the reagents. The reaction mixture was gradually warmed to 80 °C using a programmable oven over a 3 h period, held at 80 °C for 42 h and allowed to slowly cool to room temperature over 3 h. Colourless crystals were isolated by suction filtration. The crystals were washed with fresh DMF (3 × 4 mL) and air dried. Yield = 13 mg (52% based on $L-H_6$). IR (ATR): ν (cm⁻¹) = 1654, 1578, 1527, 1496, 1407, 1387, 1306, 1251, 1101, 1063, 1016, 859, 773, 726, 703, 677.

2.5. Synthesis of $[Zn_2(L-H_2)(4,4'-bipy)_2]$ (**IMP-31**)

$L-H_6$ (50 mg, 63 μmol) and $Zn(NO_3)_2 \cdot 6H_2O$ (56 mg, 87 μmol) were introduced into a screw-cap vial to which DMF (6.0 mL) was added. The mixture was agitated in an ultrasound bath for

Table 1
Crystal data and structure refinement parameters for **IMP-28–31**.

| Data | IMP-28 | IMP-29 | IMP-30 | IMP-31 |
|---|----------------------------------|---------------------------------|--------------------------------|---------------------------------|
| CCDC | 1849733 | 1849734 | 1849735 | 1849736 |
| Formula | $C_{25}H_{23}NO_{8.5}SiCd_{1.5}$ | $C_{48}H_{42}N_2O_{17}Si_2Ce_2$ | $C_{48}H_{42}N_2O_{17}Si_2Y_2$ | $C_{62}H_{42}N_4O_{13}Si_2Zn_2$ |
| Solvent | $(C_4H_9NO)(H_2O)_2$ | $(C_3H_7NO)_4(H_2O)_2$ | $(C_3H_7NO)_{5.5}$ | $(C_3H_7NO)_4$ |
| Formula Weight | 793.29 | 1583.67 | 1518.31 | 1528.28 |
| Color, habit | colourless needle | colourless prism | colourless prism | colourless block |
| Crystal size/mm ³ | 0.31 × 0.14 × 0.08 | 0.06 × 0.04 × 0.02 | 0.18 × 0.08 × 0.05 | 0.23 × 0.10 × 0.03 |
| T/K | 173(2) | 100(2) | 100(2) | 100(2) |
| Crystal system | orthorhombic | monoclinic | triclinic | triclinic |
| Space group | <i>Pnna</i> | <i>C2/c</i> | <i>P1</i> | <i>P1</i> |
| <i>a</i> (Å) | 24.5963(13) | 20.2964(4) | 11.9554(5) | 9.6743(2) |
| <i>b</i> (Å) | 19.7681(10) | 15.6880(2) | 13.5164(5) | 14.8837(3) |
| <i>c</i> (Å) | 13.7469(7) | 25.5029(4) | 14.1159(3) | 16.6832(4) |
| α (°) | 90 | 90 | 64.450(3) | 104.006(2) |
| β (°) | 90 | 109.198(2) | 75.088(3) | 105.231(2) |
| γ (°) | 90 | 90 | 79.783(3) | 99.604(2) |
| <i>V</i> (Å ³) | 6684.0(6) | 7668.8(2) | 1982.90(13) | 2179.73(9) |
| <i>Z</i> | 8 | 4 | 1 | 1 |
| <i>D</i> _{calc} (g cm ⁻³) | 1.577 | 1.372 | 1.271 | 1.164 |
| Radiation used | Cu $K\alpha$ | Mo $K\alpha$ | Cu $K\alpha$ | Mo $K\alpha$ |
| μ (mm ⁻¹) | 1.533 | 1.274 | 2.832 | 0.640 |
| 2 θ max (°) | 146 | 54 | 140 | 54 |
| No. of unique reflections | | | | |
| Measured | 6498 | 8799 | 7438 | 9934 |
| Observed [$ F_o > 4\sigma(F_o)$] | 5406 | 6547 | 4868 | 7988 |
| No. of variables | 383 | 419 | 622 | 699 |
| <i>R</i> ₁ (obs), <i>wR</i> ₂ (all) | 0.1134, 0.2690 | 0.0464, 0.1505 | 0.0876, 0.2743 | 0.0676, 0.2105 |

approximately 2 min with intermittent shaking to ensure complete dissolution of the reagents. The reaction mixture was gradually warmed to 85 °C using a programmable oven over a 3 h period, held at 85 °C for 42 h and allowed to slowly cool to room temperature over 3 h. Colourless crystals were isolated by suction filtration. The crystals were washed with fresh DMF (3 × 4 mL) and air dried. Yield = 77 mg (60% based on **L-H₆**). IR (ATR): ν (cm⁻¹) = 1667, 1611, 1541, 1495, 1415, 1387, 1369, 1256, 1223, 1104, 1073, 1017, 851, 816, 773, 753, 733, 707.

3. Results and discussion

3.1. Characterisation of [Cd₃(**L**)(DMA)₂(H₂O)₂] (**IMP-28**)

Reaction of **L-H₆** with Cd(NO₃)₂·4H₂O in a 1:1 mixture of DMA/H₂O at 85 °C in a sealed vial for 2 days afforded colourless needle crystals of **IMP-28**, where IMP is short for Imperial College London. These crystals were determined by single crystal X-ray analysis to be [Cd₃(**L**)(DMA)₂(H₂O)₂] comprising a 3D-connected MOF built from discrete trinuclear Cd-based nodes linked together by the fully deprotonated ligand **L** (Fig. 2).

IMP-28 crystallizes in the orthorhombic space group *Pnna* (no. 52) and the asymmetric unit contains half a fully-deprotonated ligand **L**, 1.5 Cd atoms, one coordinating DMA molecule and one coordinating H₂O molecule. There is some disorder in the structure with one of the phenyl rings expressing an alternative rotational position, an alternative orientation of the coordinating DMA mole-

cules and small variation in the position of Cd1 (see ESI for further information). For clarity, only the major occupancy orientations are discussed in the following analysis. Using the SQUEEZE routine of PLATON [40], it has been estimated that the pores in the framework contain two molecules of water and one molecule of DMA per asymmetric unit to give an overall formula of Cd₃(**L**)(DMA)₂(H₂O)₂·2DMA·4H₂O.

The siloxane linkage in the ligand is near linear [\angle Si–O–Si 179.3 (6)°] with staggered aryl groups, resulting in the six carboxylate branches being arranged in a *pseudo*-octahedral disposition as seen previously in **IMP-18** [33] and in the other new MOFs described in this paper. Each of the six carboxylate groups in **L** bind to a different metal node and thus the linker can be considered to be 6-connected. The trimetallic secondary building unit (SBU) present in the structure consists of three Cd(II) ions bridged by two μ_2 - η^2 : η^1 and two dimonodentate (μ_2 - η^1 : η^1) carboxylate groups (as shown in Fig. 2) with Cd–O distances lying in the range 2.204 (6)–2.487(7) Å (mean 2.301 Å). The two remaining positions on the central hexacoordinate Cd(II) atoms are filled by two coordinating DMA molecules (Cd–O = 2.179(15) Å). The terminal Cd(II) ions are further coordinated each by a chelating (η^2) carboxylate group (with Cd–O distances of 2.205(8) and 2.487(8) Å) and a coordinating H₂O molecule (Cd–O = 2.215(11) Å). Each of these coordinating carboxylate groups belong to distinct molecules of **L** and thus this SBU can be regarded as 6-connected.

In order to better understand the framework topology of **IMP-28**, the Cd₃ SBU can be simplified to a distorted trigonal prismatic 6-c node and **L** can be reduced to an octahedral 6-c point node to

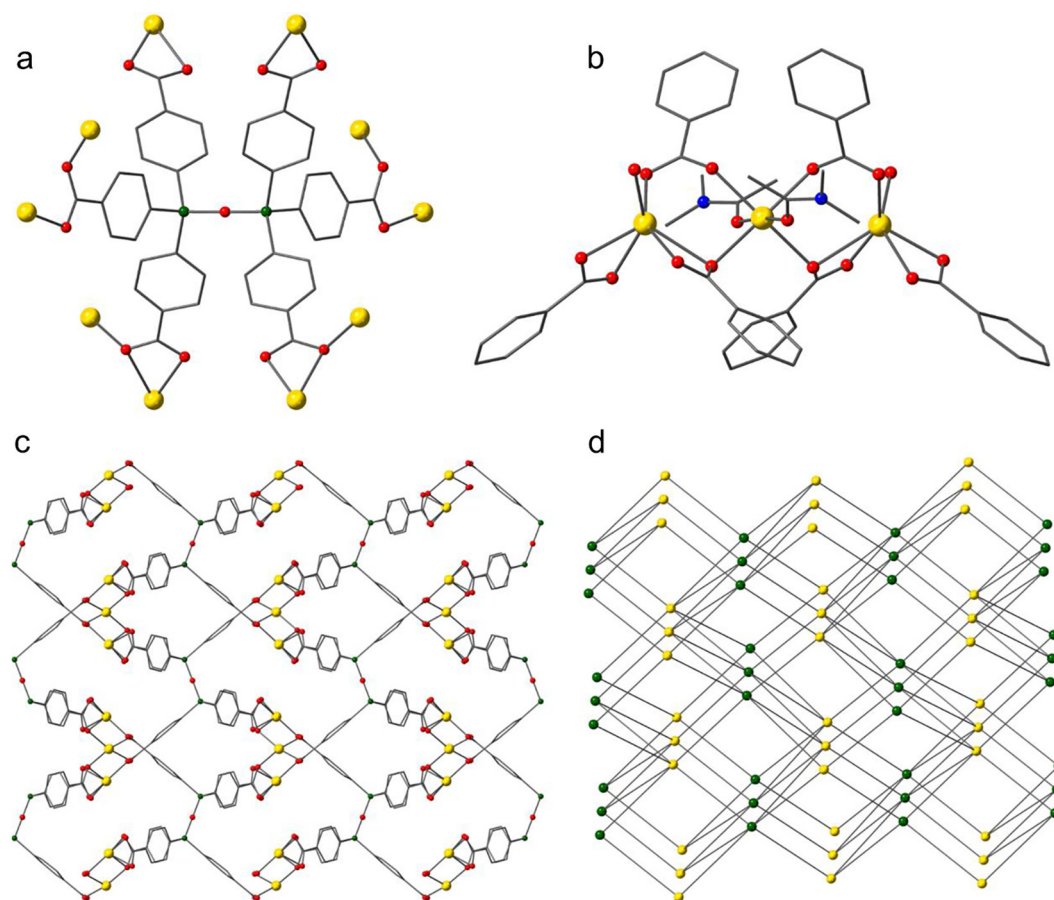


Fig. 2. (a) Coordination environment of **L** in **IMP-28**. (b) Arrangement of trinuclear cadmium cluster SBUs in **IMP-28**. (c) Section of **IMP-28** viewed down the crystallographic c axis – disorder, solvent molecules and hydrogen atoms omitted for clarity. Colour scheme: Cd, gold; O, red; C, grey; Si, green; N, blue. (d) Schematic representation of the **nia** network showing the 6-connected Cd SBU nodes (gold) and the 6-connected silicon-based nodes (green). (Colour online.)

give overall the (6,6)-c **nia** basic net as shown in Fig. 2. MOFs with the **nia** topology remain scarce in the literature though some examples are known with other hexacarboxylate linkers [42–45]. An alternative topological description for **IMP-28** in which the 6-c ligand based vertex is replaced by two 4-c silicon centred vertices, however, gives the **nia**-derived **xby** topology, rarely encountered in MOFs; see also Fig. S3.

The **IMP-28** framework has solvent-filled channels along the crystallographic *b* direction with a cross section of approximately $5 \times 5 \text{ \AA}^2$. After theoretical removal of both the coordinated and non-coordinated solvent, PLATON [40] estimates the solvent-accessible void volume for **IMP-28** to be 3567 \AA^3 or 53.4% of the unit cell volume. PXRD analysis of the bulk sample revealed peaks assignable to **IMP-28** as the main product, however the additional presence of a number of unassigned peaks indicated the presence of an impurity which we have been unable to identify (see Fig. S4). Nevertheless, evacuation of the bulk material was attempted but this led to its decomposition and a complete loss of porosity.

3.2. Characterisation of $[\text{Ce}_2(\text{L})(\text{DMF})_2(\text{H}_2\text{O})_2]$ (**IMP-29**)

Reaction of **L**-H₆ with $\text{CeCl}_3 \cdot 7\text{H}_2\text{O}$ in a 4:1 mixture of DMF/ H_2O at 80°C in a sealed vial for 2 days afforded colourless prism crystals of **IMP-29**. These crystals were characterised by single crystal X-ray analysis to be $[\text{Ce}_2(\text{L})(\text{DMF})_2(\text{H}_2\text{O})_2]$ [46]. The crystals were

found to comprise a 3D-connected MOF built from discrete bimetallic Ce-based nodes linked together by the fully deprotonated ligand **L** (Fig. 3).

IMP-29 crystallizes in the monoclinic space group $C2/c$ (no. 15) and the asymmetric unit contains half a fully-deprotonated ligand **L**, one Ce ion, one coordinating DMF molecule and one coordinating H_2O molecule. There is disorder of the central siloxane oxygen atoms about a 2-fold axis and in the orientation of the coordinating DMF molecules (see ESI for further information). For clarity, only the major occupancy orientations are discussed in the following analysis. Using the solvent masking routine of Olex-2 [38], it has been estimated that the pores in the framework contain two molecules of water and four molecules of DMF per asymmetric unit to give an overall formula of $[\text{Ce}_2(\text{L})(\text{DMF})_2(\text{H}_2\text{O})_2] \cdot 4\text{DMF} \cdot 2\text{H}_2\text{O}$.

The siloxane linkage in the connector is near linear [Si-O-Si $169(2)^\circ$] with the six carboxylate branches disposed in an octahedral manner. Each of the six carboxylate groups in **L** bind to a different metal node and thus the linker can be considered to be 6-connected. The bimetallic SBU present in the structure consists of two Ce(III) ions held together by two chelating/bridging carboxylates ($\mu_2\text{-}\eta^2\text{:}\eta^1$) and two bridging dimonodentate ($\mu_2\text{-}\eta^1\text{:}\eta^1$) carboxylate groups (as shown in Fig. 3) with Ce–O distances lying in the range $2.425(3)\text{--}2.899(3) \text{ \AA}$ (mean 2.541 \AA). The Ce(III) ions are further coordinated each by a chelating (η^2) carboxylate group (with Ce–O distances of $2.549(3)$ and $2.551(3) \text{ \AA}$), a coordinating DMF molecule (Ce–O = $2.497(10) \text{ \AA}$) and a coordinating H_2O mole-

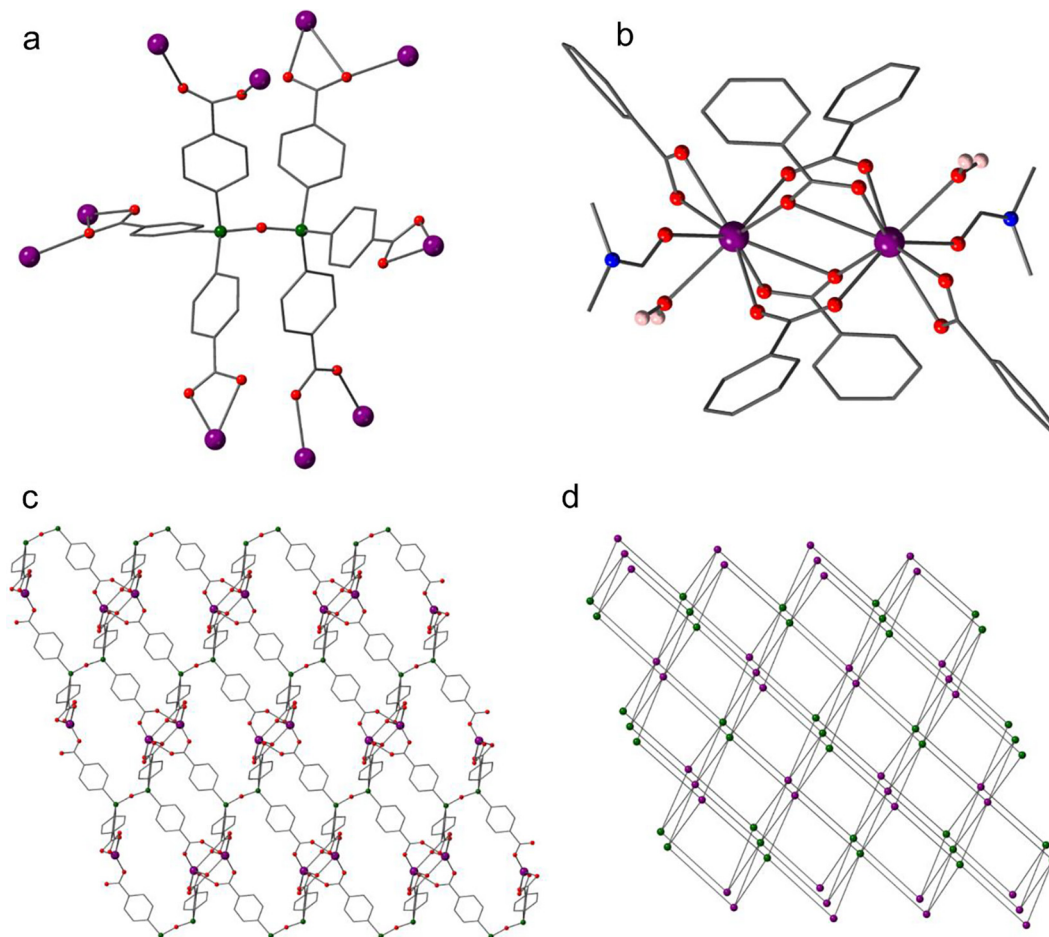


Fig. 3. (a) Coordination environment of **L** in **IMP-29**. (b) Arrangement of dinuclear cerium cluster SBUs in **IMP-29**. (c) Section of **IMP-29** viewed down the crystallographic *b* axis – disorder, solvent molecules and hydrogen atoms omitted for clarity. Colour scheme: Ce, purple; O, red; C, grey; Si, green; N, blue; hydrogen, pink. (d) Schematic representation of the **pcu** network showing the 6-connected Ce SBU nodes (purple) and the 6-connected silicon-based nodes (green). (Colour online.)

cule ($\text{Ce}-\text{O} = 2.537(4) \text{ \AA}$). Each of these coordinating carboxylate groups belong to distinct molecules of **L** and thus the overall geometry of this SBU is a 6-connected distorted octahedron.

Looking closely at the framework topology of **IMP-29**, both the Ce_2 SBU and **L** ligand can be reduced to pseudo-octahedral 6-c point nodes to give the well-known 6-c **pcu** basic net as shown in Fig. 3. An alternative topological description in which the 6-c ligand based vertex is replaced by two 4-c silicon centred vertices, however, gives the less commonly encountered 4,6-c **fsh** topology [47–49]; see also Fig. S7.

The **IMP-29** framework has solvent-filled channels with the largest window size being ca. $6 \times 8 \text{ \AA}^2$ in the 110 crystallographic direction. After theoretical removal of both the coordinated and non-coordinated solvent, PLATON [40] estimates the solvent-accessible void volume for **IMP-29** to be 4446 \AA^3 or 58.0% of the unit cell volume. PXRD measurements on a bulk sample of **IMP-29**, however, suggested its decomposition during isolation and drying procedures.

3.3. Characterisation of $[\text{Y}_2(\text{L})(\text{DMF})_2(\text{H}_2\text{O})_2]$ (**IMP-30**)

Reaction of **L-H**₆ with $\text{Y}(\text{NO}_3)_3 \cdot 6\text{H}_2\text{O}$ in a 4:1 mixture of DMF/ H_2O at 80°C in a sealed vial for 2 days afforded colourless prism crystals of **IMP-30**. These crystals were characterised by single crystal X-ray analysis to be $[\text{Y}_2(\text{L})(\text{DMF})_2(\text{H}_2\text{O})_2]$. The crystals were found to comprise a 3D-connected MOF built from discrete bimetallic Y-based nodes linked together by the fully deprotonated ligand **L** (Fig. 4).

IMP-30 crystallizes in the triclinic space group $P\bar{1}$ (no. 2) and the asymmetric unit contains half a fully-deprotonated ligand **L**, one Y ion, one coordinating DMF molecule and one coordinating H_2O molecule. The orientation of the ligand **L** in the structure is disordered over two orientations with 63:37 occupancy. The relative orientations of the ligand share a fixed central oxygen and are related by a roughly 69° rotation. Despite this, both arrangements result in six coordinating carboxylate groups being in approximately the same positions, allowing the Y(III) ions to remain in a fixed position within the lattice. There is also disorder in the orientation of the coordinating DMF molecules (see ESI for further information). For clarity only the major occupancy orientations are discussed here. Using the solvent masking routine of Olex-2 [38], it has been estimated that the pores in the framework contain 5.5 molecules of DMF per asymmetric unit to give an overall formula of $[\text{Y}_2(\text{L})(\text{DMF})_2(\text{H}_2\text{O})_2] \cdot 5.5\text{DMF}$.

The siloxane linkage in the ligand is linear [$\text{Si}-\text{O}-\text{Si}$ 180.0°] (the central siloxane oxygen sits on a centre of symmetry) with the six carboxylate branches disposed in an octahedral manner. Each of the six carboxylate groups in **L** bind to a different metal node and thus the linker can be considered to be 6-connected. The bimetallic SBU present in the structure consists of two Y(III) ions held together by two bridging dimonodentate ($\mu_2-\eta^1:\eta^1$) carboxylate groups (as shown in Fig. 4) with Y–O distances of 2.220 (11) and 2.300(14) Å. The Y(III) ions are further coordinated each by two chelating (η^2) carboxylate groups (with Y–O distances lying in the range 2.404(13)–2.482(18) Å, mean 2.444 Å), a coordinating DMF molecule (Y–O = 2.186(10) Å) and a coordinating H_2O molecule (Y–O = 2.314(6) Å). Each of these coordinating carboxy-

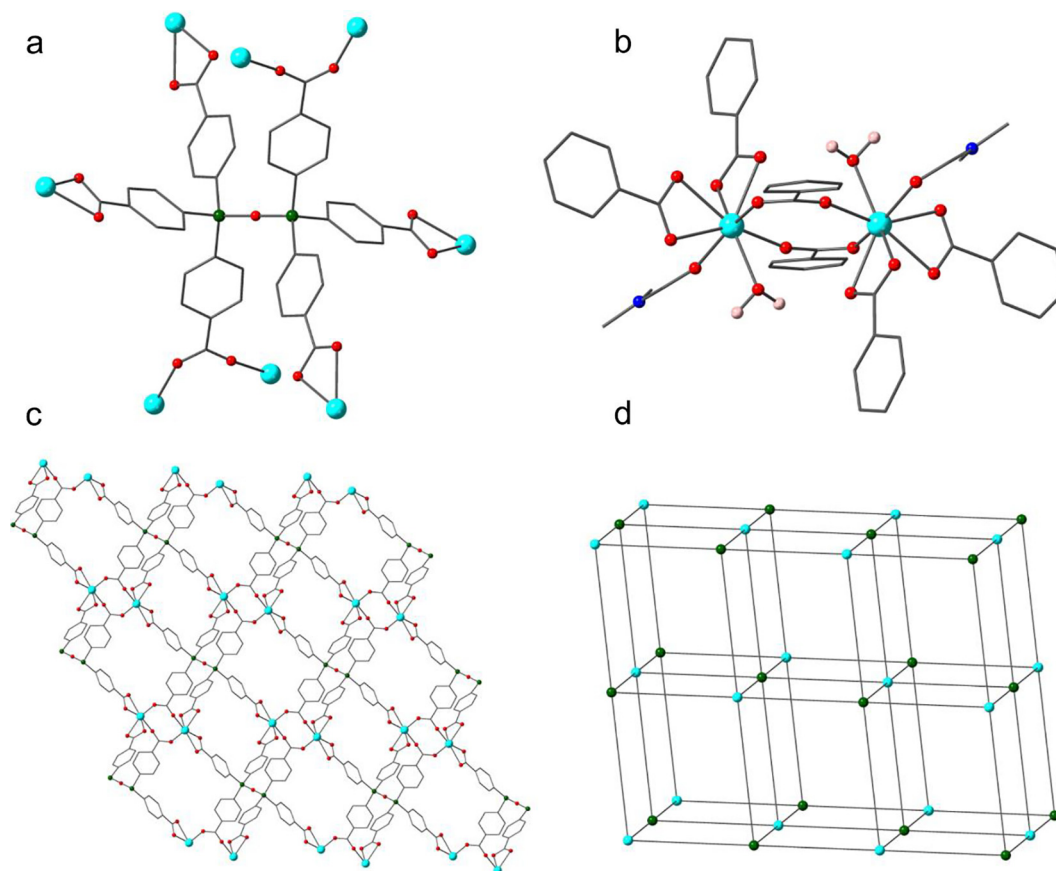


Fig. 4. (a) Coordination environment of **L** in **IMP-30**. (b) Arrangement of dinuclear yttrium cluster SBUs in **IMP-30**. (c) Section of **IMP-30** viewed down the crystallographic *a* axis – disorder, solvent molecules and hydrogen atoms omitted for clarity. Colour scheme: Y, cyan; O, red; C, grey; Si, green; N, blue; hydrogen, pink. (d) Schematic representation of the **pcu** network showing the 6-connected Y SBU nodes (cyan) and the 6-connected silicon-based nodes (green). (Colour online.)

late groups belong to distinct molecules of **L** and thus the overall geometry of this SBU is a 6-connected distorted octahedron.

Looking closely at the framework topology of **IMP-30**, both the bimetallic Y_2 SBU and **L** ligand can be reduced to pseudo-octahedral 6-c point nodes to give a 6-c **pcu** basic net as shown in Fig. 4. Thus, while **IMP-29** and **IMP-30** are not isostructural crystallographically, from a topological point of view they both have the same connectivity of their underlying nets. The major difference between the two systems is in the geometry of the deconstructed metallic nodes; **IMP-29** displays a higher degree of distortion away from the ideal octahedral geometry of the metal-based 6-c vertex. An alternative topological description of **IMP-30** in which the 6-c ligand node is replaced by two 4-c vertices (centred on the terminal silicon atoms of **L**) gives the 4,6-c **fsh** topology as seen in **IMP-29**; see also Fig. S11.

The **IMP-30** framework has solvent-filled channels with the largest window size being ca. $6 \times 8 \text{ \AA}^2$ in the crystallographic *c* direction. After theoretical removal of both the coordinated and non-coordinated solvent, PLATON [40] estimates the solvent-accessible void volume for **IMP-30** to be 1186.4 \AA^3 or 59.8% of the unit cell volume. As seen with **IMP-29**, attempted PXRD measurements on bulk samples of **IMP-30** after isolation and air drying suggested its decomposition during isolation and drying procedures.

3.4. Characterisation of $[\text{Zn}_2(\text{LH}_2)(4,4'\text{-bipy})_2]$ (**IMP-31**)

Reaction of **L-H**₆ with $\text{Zn}(\text{NO}_3)_2 \cdot 6\text{H}_2\text{O}$ and 4,4'-bipyridine in DMF at 80°C in a sealed vial for 2 days afforded colourless block crystals of **IMP-31**. These crystals were characterised by single crystal X-ray analysis to be $[\text{Zn}_2(\text{LH}_2)(4,4'\text{-bipy})_2]$. The crystals were found to comprise a doubly interpenetrated (see Fig. S17) 3D-connected MOF built from mononuclear $\text{Zn}(\text{II})$ nodes linked together by the quadruply deprotonated ligand **LH**₂ (Fig. 5) and the neutral linker 4,4'-bipyridine.

IMP-31 crystallizes in the triclinic space group $P\bar{1}$ (no. 2) and the asymmetric unit contains half a tetra-anionic ligand **LH**₂, one $\text{Zn}(\text{II})$ ion, and two distinct halves of 4,4'-bipyridine linkers. The orientation of the ligand **LH**₂ in the structure is disordered over two orientations with 79:21 occupancy. The relative orientations of the ligand share a fixed central oxygen and are related by a 81° rotation. Despite this, both arrangements result in the coordinating carboxylate groups being in approximately the same positions, allowing the $\text{Zn}(\text{II})$ ions to remain in a fixed position within the lattice. There is further positional disorder of the non-coordinating carboxylate groups (see ESI for further information). For clarity in the discussion only the major occupancy orientation of each case is discussed. Using the SQUEEZE routine of PLATON

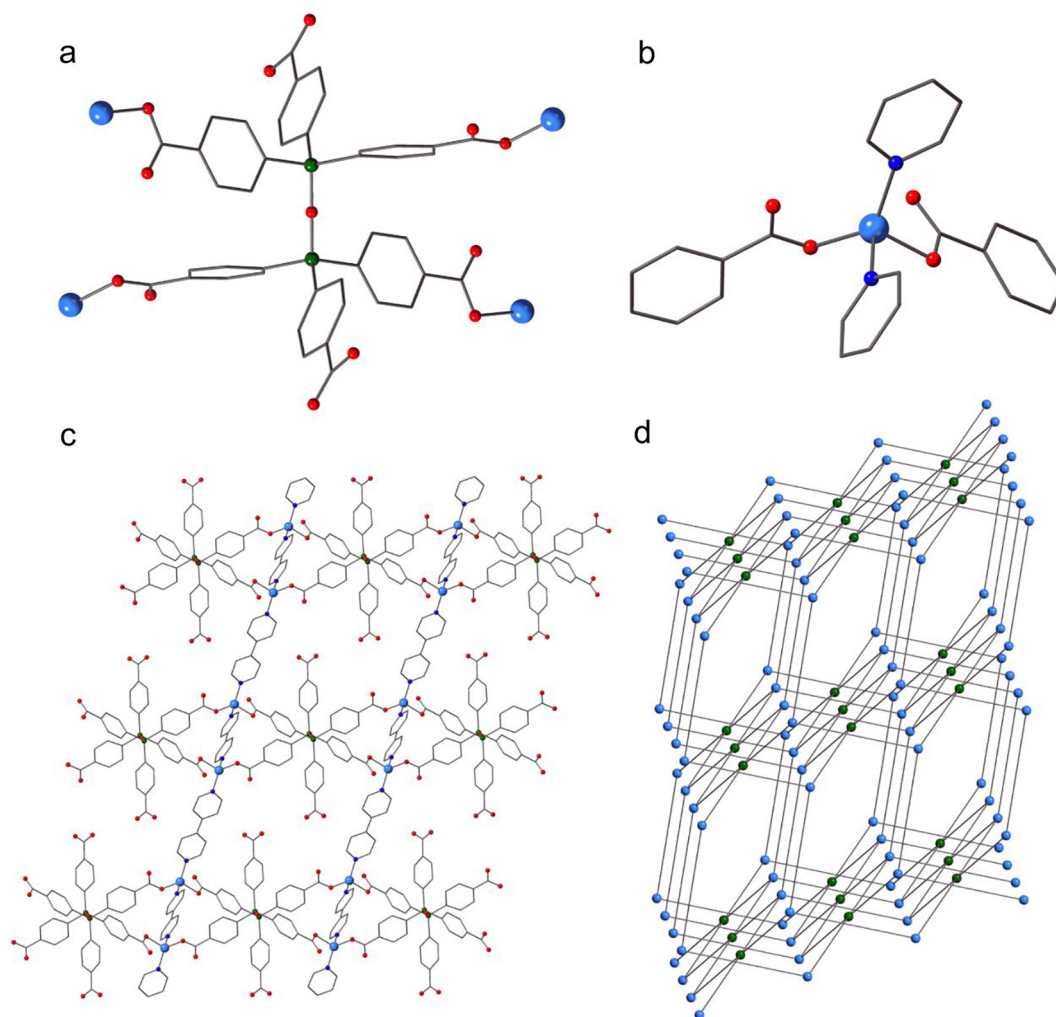


Fig. 5. (a) Coordination environment of **LH**₂ in **IMP-31**. (b) Arrangement of mononuclear zinc SBUs in **IMP-31**. (c) Section of **IMP-31** viewed down the crystallographic *a* axis – disorder, solvent molecules and hydrogen atoms omitted for clarity. Colour scheme: Zn, light blue; O, red; C, grey; Si, green; N, royal blue. (d) Schematic representation of the **mog** network showing the 4-connected Zn nodes (light blue) and the 4-connected silicon-based nodes (green) – only one of the two interpenetrating nets is shown. (Colour online.)

[40], it has been estimated that the pores in the framework contain 4 molecules of DMF per asymmetric unit to give an overall formula of $[\text{Zn}_2(\text{LH}_2)(4,4'\text{-bipy})_2]\cdot 4\text{DMF}$.

The siloxane linkage in the ligand is linear [Si-O-Si 180.0°] (the central siloxane oxygen sits on a centre of symmetry) with the six carboxylate branches disposed in an octahedral manner. Only four of the six carboxylate groups in LH_2 bind to zinc nodes and thus the linker can be considered to be 4-connected. Charge balance requires that the remaining two carboxylic acid groups (which are non-binding) are protonated and, though these protons could not be located in the crystallographic ΔF map, this is supported by the asymmetric nature of the of the C47–O41/42 bonds which show C–O distances of 1.215(10) and 1.240(11) Å, respectively. The mononuclear $\text{Zn}(\text{II})$ nodes present in the structure are coordinated by two monodentate carboxylate groups from two different LH_2 ligands and two aromatic nitrogens from two separate 4,4'-bipyridine molecules (as shown in Fig. 5). The Zn–O distances are 1.961(3) and 1.997(8) Å while the Zn–N distances are 2.028(2) and 2.102(3) Å. The overall geometry of this SBU is consequently a 4-connected distorted tetrahedron.

From a topological point of view, the LH_2 ligand can be simplified to a square planar node owing to the fact that two of its carboxylic acid groups are non-binding. The Zn-based nodes are tetrahedral with the 2-connected 4,4'-bipyridine units act as linear links between Zn vertices. Thus, the two types of 4-c nodes connect together to give the less commonly encountered 4,4-c **mog** topology [50–53] as depicted in Fig. 5. An alternative topological description in which the 4-c ligand based vertex is replaced by two 3-c silicon centred vertices, however, gives a new 3,4-c topology whose point symbol is $\{6^3\}\{6^5\cdot 8\}$ with stoichiometry (3-c)(4-c); see also Fig. S15.

The **IMP-31** framework has solvent-filled channels with the largest window size being ca. $5 \times 10 \text{ Å}^2$ in the crystallographic b direction. After theoretical removal of both the coordinated and non-coordinated solvent, PLATON [40] estimates the solvent-accessible void volume for **IMP-31** to be 987.6 Å^3 or 45.3% of the unit cell volume. PXRD of the bulk material however suggested decomposition of the **IMP-31** framework during isolation procedures thus precluding further studies on this material.

4. Conclusions

The results presented here extend our studies on the octahedral siloxane-based hexacarboxylate linker **L** for MOF construction to other d-block and f-block metals. Thus, treatment of L-H_6 with Cd^{II} , Ce^{III} , and Y^{III} salts has been demonstrated to result in the assembly of the MOF materials **IMP-28**, **IMP-29**, and **IMP-30** respectively. These novel MOFs all comprise metal-based clusters which are cross-linked by fully deprotonated molecules of **L** to afford 3D networks with solvent filled channels. Hexatopic and in particular octahedral connectors remain scarce in the literature, and thus the metal complexes of **L** presented herein display uncommon MOF topologies including **nia** and **fsh** [35]. Combining L-H_6 with Zn^{II} and 4,4'-bipyridine gave the mixed linker MOF **IMP-31** which features less commonly-encountered monoatomic Zn nodes and possesses the rare **mog** topology. Although polytopic linkers have been noted to produce MOFs of enhanced stability [54], the MOFs reported here were found to be unstable to evacuation. This is likely due to the structures of the metallic clusters in these new materials. The SBUs are of low nuclearity (≤ 3 metal ions per SBU) and linking to the organosilicon node is in many cases via coordination of a chelating carboxylate group to a terminal metal ion i.e. there are relatively few bridging carboxylates holding the clusters together. Work is ongoing in our laboratories towards preparing MOFs with **L** and more highly connected multimetallic

clusters (e.g. Zr_6O_8) which are expected to impart significantly improved stability on these systems.

Acknowledgements

The Imperial College President's Scholarship Scheme (L.D.) and the EPSRC (EP/M507878/1) are acknowledged for funding this work.

Appendix A. Supplementary data

CCDC 1849733–1849736 contains the supplementary crystallographic data for **IMP-28**–**IMP-31**. These data can be obtained free of charge via <http://www.ccdc.cam.ac.uk/conts/retrieving.html>, or from the Cambridge Crystallographic Data Centre, 12 Union Road, Cambridge CB2 1EZ, UK; fax: (+44) 1223-336-033; or e-mail: deposit@ccdc.cam.ac.uk.

Supplementary data to this article can be found online at <https://doi.org/10.1016/j.poly.2018.09.050>.

References

- [1] K.E. Cordova, O.M. Yaghi, *Mater. Chem. Front.* 1 (2017) 1304.
- [2] S. Kaskel, *The Chemistry of Metal-organic Frameworks: Synthesis, Characterization, and Applications*, John Wiley & Sons, 2016.
- [3] P.Z. Moghadam, A. Li, S.B. Wiggins, A. Tao, A.G.P. Maloney, P.A. Wood, S.C. Ward, D. Fairen-Jimenez, *Chem. Mater.* 29 (2017) 2618.
- [4] H. Furukawa, K.E. Cordova, M. O'Keeffe, O.M. Yaghi, *Science* 341 (2013) 1230444.
- [5] A.U. Czaja, N. Trukhan, U. Muller, *Chem. Soc. Rev.* 38 (2009) 1284.
- [6] F.A. Almeida Paz, J. Klinowski, S.M.F. Vilela, J.P.C. Tome, J.A.S. Cavaleiro, J. Rocha, *Chem. Soc. Rev.* 41 (2012) 1088.
- [7] R.P. Davies, R.J. Less, P.D. Lickiss, K. Robertson, A.J.P. White, *Inorg. Chem.* 47 (2008) 9958.
- [8] R.P. Davies, R. Less, P.D. Lickiss, K. Robertson, A.J.P. White, *Cryst. Growth Des.* 10 (2010) 4571.
- [9] R.P. Davies, P.D. Lickiss, K. Robertson, A.J.P. White, *Aust. J. Chem.* 64 (2011) 1239.
- [10] R.P. Davies, P.D. Lickiss, K. Robertson, A.J.P. White, *CrystEngComm* 14 (2012) 758.
- [11] I. Timokhin, J. Baguna Torres, A.J.P. White, P.D. Lickiss, C. Pettinari, R.P. Davies, *Dalton Trans.* 42 (2013) 13806.
- [12] I. Timokhin, A.J.P. White, P.D. Lickiss, C. Pettinari, R.P. Davies, *CrystEngComm* 16 (2014) 8094.
- [13] B. Sels, L. Kustov, *Zeolites and Zeolite-like Materials*, Elsevier, Amsterdam, 2016.
- [14] P. Eliasova, M. Opanasenko, P.S. Wheatley, M. Shamzhy, M. Mazur, P. Nachtigall, W.J. Roth, R.E. Morris, J. Cejka, *Chem. Soc. Rev.* 44 (2015) 7177.
- [15] R. Millini, G. Bellussi, *Catal. Sci. Technol.* 6 (2016) 2502.
- [16] P. Van Der Voort, D. Esquivel, E. De Canck, F. Goethals, I. Van Driessche, F.J. Romero-Salguero, *Chem. Soc. Rev.* 42 (2013) 3913.
- [17] J.G. Croissant, X. Cattoen, M. Wong Chi Man, J.-O. Durand, N.M. Khashab, *Nanoscale* 7 (2015) 20318.
- [18] Y. Chen, J. Shi, *Adv. Mater.* 28 (2016) 3235.
- [19] D.B. Cordes, P.D. Lickiss, F. Rataboul, *Chem. Rev.* 110 (2010) 2081.
- [20] Q. Ye, H. Zhou, J. Xu, *Chem. Asian J.* 11 (2016) 1322.
- [21] C. Racles, M.-F. Zaltariou, M. Jacob, M. Silion, M. Avadanei, A. Bargan, *Appl. Catal., B* 205 (2017) 78.
- [22] A. Vlad, M. Cazacu, M.-F. Zaltariou, S. Shova, C. Turta, A. Airinei, *Polymer* 54 (2013) 43.
- [23] A. Vlad, M. Cazacu, M.-F. Zaltariou, A. Bargan, S. Shova, C. Turta, *J. Mol. Struct.* 1060 (2014) 94.
- [24] M.S. Deshmukh, T. Vijayakanth, R. Boomishankar, *Inorg. Chem.* 55 (2016) 3098.
- [25] M.-F. Zaltariou, M. Cazacu, L. Sacarescu, A. Vlad, G. Novitchi, C. Train, S. Shova, V.B. Arion, *Macromolecules* 49 (2016) 6163.
- [26] A. Vlad, M.-F. Zaltariou, S. Shova, G. Novitchi, C.-D. Varganici, C. Train, M. Cazacu, *CrystEngComm* 15 (2013) 5368.
- [27] E. Carbonell, L.A. Bivona, L. Fusaro, C. Aprile, *Inorg. Chem.* 56 (2017) 6393.
- [28] A.C. Kucuk, J. Matsui, T. Miyashita, *RSC Adv.* 8 (2018) 2148.
- [29] S. Banerjee, S. Kataoka, T. Takahashi, Y. Kamimura, K. Suzuki, K. Sato, A. Endo, *Dalton Trans.* 45 (2016) 17082.
- [30] D.M.L. Goodgame, S. Kealey, P.D. Lickiss, A.J.P. White, *J. Mol. Struct.* 890 (2008) 232.
- [31] M.T. Hay, B. Seurer, D. Holmes, A. Lee, *Macromolecules* 43 (2010) 2108.
- [32] M. Cazacu, A. Airinei, M. Marcu, *Appl. Organomet. Chem.* 16 (2002) 643.
- [33] L.C. Delmas, P.N. Horton, A.J.P. White, S.J. Coles, P.D. Lickiss, R.P. Davies, *Chem. Commun.* 53 (2017) 12524.

- [34] A. Raghuvanshi, C. Strohmann, J.-B. Tissot, S. Clément, A. Mehdi, S. Richeter, L. Viau, M. Knorr, *Chem. Eur. J.* 23 (2017) 16479.
- [35] M. Li, D. Li, M. O'Keeffe, O.M. Yaghi, *Chem. Rev.* 114 (2014) 1343.
- [36] G. Sheldrick, *Acta Crystallogr. Sect. C: Cryst. Struct. Commun.* 71 (2015) 3.
- [37] G. Sheldrick, *Acta Crystallogr. Sect. A: Found. Crystallogr.* 71 (2015) 3.
- [38] O.V. Dolomanov, L.J. Bourhis, R.J. Gildea, J.A.K. Howard, H. Puschmann, *J. Appl. Crystallogr.* 42 (2009) 339.
- [39] L. Farrugia, *J. Appl. Crystallogr.* 45 (2012) 849.
- [40] A.L. Spek, *J. Appl. Crystallogr.* 36 (2003) 7.
- [41] D. Palmer, *CrystalMaker X for Win64 V10.1.1*, CrystalMaker Software Limited, Oxfordshire, England, 2009.
- [42] K. Liu, Y. Sun, H. Hu, L. Wang, *Polyhedron* 131 (2017) 8.
- [43] K. Liu, X. Li, D. Ma, Y. Han, B. Li, Z. Shi, Z. Li, L. Wang, *Mater. Chem. Front.* 1 (2017) 1982.
- [44] J. Jia, F. Sun, T. Borjigin, H. Ren, T. Zhang, Z. Bian, L. Gao, G. Zhu, *Chem. Commun.* 48 (2012) 6010.
- [45] H.K. Chae, M. Eddaoudi, J. Kim, S.I. Hauck, J.F. Hartwig, M. O'Keeffe, O.M. Yaghi, *J. Am. Chem. Soc.* 123 (2001) 11482.
- [46] S.J. Coles, P.A. Gale, *Chem. Sci.* 3 (2012) 683.
- [47] F. Guo, F. Wang, H. Yang, X. Zhang, J. Zhang, *Inorg. Chem.* 51 (2012) 9677.
- [48] D. Davarci, R. Gur, S. Besli, E. Senkuytu, Y. Zorlu, *Acta Crystallogr. Sect. B: Struct. Sci.* 72 (2016) 344.
- [49] L. Luan, J. Li, C. Chen, Z. Lin, H. Huang, *Inorg. Chem.* 54 (2015) 9387.
- [50] F. Wei, Y. Ye, W. Huang, Q. Lin, Z. Li, L. Liu, S. Chen, Z. Zhang, S. Xiang, *Inorg. Chem. Commun.* 93 (2018) 105.
- [51] S.-L. Cai, X.-L. Huang, Z.-H. He, H.-M. Lin, S.-R. Zheng, W.-G. Zhang, *J. Chem. Crystallogr.* 48 (2018) 47.
- [52] W. Jiang, J. Yang, Y.-Y. Liu, S.-Y. Song, J.-F. Ma, *Inorg. Chem.* 56 (2017) 3036.
- [53] L. Liu, C. Huang, X. Xue, M. Li, H. Hou, Y. Fan, *Cryst. Growth Des.* 15 (2015) 4507.
- [54] S. Yuan, L. Feng, K. Wang, J. Pang, M. Bosch, C. Lollar, Y. Sun, J. Qin, X. Yang, P. Zhang, Q. Wang, L. Zou, Y. Zhang, L. Zhang, Y. Fang, J. Li, H.-C. Zhou, *Adv. Mater.* 30 (2018) 1704303, <https://doi.org/10.1002/adma.201704303>.